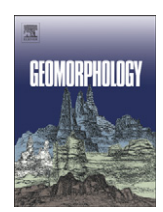
ELSEVIER

Contents lists available at ScienceDirect

# Geomorphology

journal homepage: www.elsevier.com/locate/geomorph



# Modelling karst geomorphology on different time scales

## Georg Kaufmann

Institute of Geological Sciences, Geophysics Section, Free University of Berlin, Malteserstr. 74-100, Haus D, 12249 Berlin, Germany

#### ARTICLE INFO

Article history: Accepted 18 September 2008 Available online 8 October 2008

Keywords: Karst Limestone Dissolution Aquifer

#### ABSTRACT

The evolution and flow in a karst aquifer is studied with numerical simulations, based on the KARST model (Karst AquifeR Simulation Tool). The aquifer consists of a three-dimensional interconnected network of conduits representing fractures in the rock, and a porous rock matrix representing the finer fissured system in the rock. Flow through the aquifer can be driven by both diffuse recharge from precipitation and localised sinking streams, and the aquifer drains towards a large karst resurgence representing the base level. Superimposed onto the karst aquifer is a landscape, which can evolve with time by small-scale diffusive processes, large-scale river erosion, and karst denudation.

Fractures in the aquifer are enlarged with time by chemical dissolution, enhancing the secondary porosity of the karst aquifer. The enlargement of fractures results in a dramatic increase of the aquifer conductivity over several orders of magnitude, and a change of flow patterns from an initially pore-controlled to a heterogeneous fracture-controlled aquifer. During the evolution, the water table is falling from an initially high position close to the land surface to a lower level coinciding with the actual base level.

Two model scenarios are studied to elucidate the karst aquifer evolution in three dimensions. The evolution models are then complemented by event-type spring discharge modelling, which can be used as a predictive tool for karst spring discharge and contaminant transport.

© 2008 Elsevier B.V. All rights reserved.

#### 1. Introduction

Groundwater flow in a karst aquifer is an important subject, as rapid flow of water through highly permeable karst aquifers is prone to contamination. However, large-scale heterogeneities in the karst aquifer make it difficult to predict flow and transport in a karst catchment. While the primary conductivity of limestone is fairly low ( $K \sim 10^{-8} \text{ m s}^{-1}$ ), fractures in the rock enlarged by chemical dissolution increase their conductivity by orders of magnitude (K > 1–  $10 \text{ m s}^{-1}$ , see also Table 1). The enlargement of initially small fractures into larger passages then forms a pattern of cave passages, which carry the majority of water flowing through the karst aquifer. The *shortterm response* of a karst aquifer observed today is guided by the *longterm evolution* of secondary porosity within the karst aquifer. Hence we need to discuss both long-term evolution and short-term response to understand the complicated dynamics of a karst aquifer.

### 1.1. Aquifer geometry

Palmer (1991) has analysed several thousand cave passage patterns and found that 57% of the total cave passages follow bedding planes and 42% are fracture-oriented. Only 1% of the total passages are related to intergranular porosity in the rock. In his classification, Palmer (1991) introduced four distinct patterns of cave passages:

(i) Branchwork caves (65% of total passage length), resembling single passages joining larger passages downstream as tributaries and thus similar to surficial dentritic river patterns. (ii) Network caves (17%), with passage patterns of angular grids formed by dissolutional enlargement of most of the available fractures. (iii) Anastomotic caves (10%), with patterns of intersecting, curvilinear tubes, often superimposed on branchwork caves. (iv) Ramiform and spongework caves (8%), with random-like patterns of small cavities and larger, irregular rooms, mainly resulting from hydrothermally controlled dissolution and therefore not directly related to surface recharge. Examples for the first two cave passage patterns are shown in Fig. 1.

The *Nandembo Cave System* in the Matumbi Hills, Tanzania (Laumanns and Ruggieri, 1995), a 7.5km long active river cave with three independent tributaries, is an example of a branchwork pattern. The system is recharged via sinking streams, and drains towards a single karst resurgence.

Anjohiambovonomby cave in Namoroka, Madagascar (Laumanns and Gebauer, 1993), a maze cave with a total length of 4.6km, is a typical example of a network pattern. The cave is located in a karst outcrop, recharge is entirely diffusive over the entire surface, and water emerges in an overflow spring active only during the rainy season.

These widely different cave passage patterns pose the important question of identifying the characteristic processes responsible for the different evolution. We need to answer questions such as 'how important is the recharge condition', 'is the structural setting guiding the evolution', 'is water chemistry decisive in the long-term evolution'. Here, numerical simulations of long-term karst aquifer

E-mail address: georg.kaufmann@fu-berlin.de.

**Table 1**Reference model parameters

Parameter	Description	Unit	Value
Climate			
$T_{c}$	Temperature	°C	10
P	Carbon dioxide pressure	atm	0.05
N	Precipitation	mm/yr	> GW R
GW R	Groundwater recharge	mm/yr	600
Equilibrium chemistry			
T	Temperature	°K	273.16+T <sub>c</sub>
I	Ion activity	mol l <sup>-1</sup>	3 <i>c</i>
Aª	Debye-Hückel coefficient	_	$0.4883 + 8.074 \times 10^{-4}T_{c}$
B <sup>a</sup>	Debye-Hückel coefficient	_	$0.3241 + 1.600 \times 10^{-4}T_{c}$
$\log \gamma_{Ca^{2+}}^{b}$	Activity coefficient	_	-4A√Ī
0,1	·		$\frac{4I\sqrt{I}}{1+5.0B\sqrt{I}}$
logγ <sub>HCO3</sub> -b	Activity coefficient	_	$-1A\sqrt{I}$
108 / ncu <sub>3</sub>	rearry coemercia		<u></u> _
			$1+5.4B\sqrt{I}$
$\log K_0$	Equilibrium constant	-	$K_5/K_1$
$\log K_1^c$	Equilibrium constant	mol l <sup>-1</sup>	-356.3094-0.06091964T
			+21834.37 / T + 126.8339 log T
			-1684915/T <sup>b</sup>
$\log K_2^c$	Equilibrium constant	mol l <sup>-1</sup>	-107.8871 -0.03252849T
			+5151.79/T+38.92561 log T
			-563713.9/T <sup>b</sup>
log K5 <sup>c</sup>	Equilibrium constant	mol l <sup>-1</sup>	1.707×10 <sup>-4</sup>
$\log K_{\rm C}^{\rm c}$	Equilibrium constant	mol <sup>2</sup> l <sup>-2</sup>	-171.9065-0.077993 <i>T</i>
	-		+2839.319/T+71.595 log T
$\log K_{\rm H}^{\rm c}$	Equilibrium constant	mol l <sup>-1</sup> atm <sup>-1</sup>	108.3865 + 0.01985076T
	•		-6919.53 /T-40.45154 log T
			+669365/T <sup>b</sup>
F1			
Fluxrates	x 200 x 20		
$n_0$	Initial linear exponent	-	1
$n_1$	Slow linear exponent	-	1
$n_2$	High-order exponent	-	4
$m_0$	Initial intercept	-	0.3
$m_1$	Slow intercept	-	1
$m_2$	High-order intercept	-	1
$k_0$	Initial rate constant	mol/m²/s	$4 \times 10^{-6}$
$k'_1$	Slow rate constant	mol/m²/s	$4 \times 10^{-7}$
k <sub>2</sub>	High-order rate constant	mol/m²/s	Eq. (5)
D	Diffusion constant	m <sup>2</sup> /s	10 <sup>-9</sup>
$C_i$	Initial calcium concentration		0–2
$c_0$	Threshold calcium	mol/m <sup>3</sup>	$0.3c_{\rm eq}$
	concentration	1/ 2	0.0
$c_1$	Threshold calcium	mol/m <sup>3</sup>	$0.9c_{\mathrm{eq}}$
	concentration	., 3	T (4)
$c_{ m eq}$	Equilibrium calcium	mol/m <sup>3</sup>	Eq. (1)
	concentration		
Conduit			
d	Fracture diameter	m	
h	Hydraulic head	m	
Q	Flow rate	m <sup>3</sup> /s	
Q Re	Reynolds number	111 /5	
	Friction factor		
$f_i$		m	0.00002
w	Wall roughness	m	0.00002

- <sup>a</sup> From Truesdell and Jones (1974).
- <sup>b</sup> From Robinson and Stokes (1955).
- <sup>c</sup> From Plummer and Busenberg (1982).

evolution both in terms of flow and geometry have been used intensely during recent years (Dreybrodt, 1990; Palmer, 1991; Groves and Howard, 1994a,b; Howard and Groves, 1995; Clemens et al., 1996; Clemens et al., 1997; Hanna and Rajaram, 1998; Siemers and Dreybrodt, 1998; Kaufmann and Braun, 1999, 2000; Gabrovšek and Dreybrodt, 2000, 2001; Bauer et al., 2002; Bauer et al., 2003; Romanov et al., 2002; Romanov et al., 2003; Kaufmann, 2002a,b, 2003a,b, 2005; Dreybrodt et al., 2005). Common to all of these numerical models is the change from an initially relatively homogeneous aquifer with small fractures, where flowrates are low and flow is diffuse, to a strongly heterogeneous aquifer with flow being

fast and concentrated along enlarged fractures. Often, a preferential flowpath is established in the models, which guides recharge through cave passages towards a karst spring.

#### 1.2. Aquifer response

The large variability in karst aquifer properties cannot be observed properly by field measurements, as typical methods such as injection, packer, and slug tests are more suitable to porous groundwater flow. Flow in the enlarged fracture system is, however, more difficult to estimate. Only in a few cases it is possible to explore the enlarged fracture system directly. Hence, the prediction of flow and contamination needs to be studied by other means.

A global observation of the response of a karst aquifer is hydrographs taken from large karst springs. These resurgences often collect water from the entire catchment area and show a rapid response to sudden recharge events, followed by an exponential decrease of discharge seen along the recession limb of the hydrograph. As an example, a four-month long hydrograph reading from the Gallusquelle in southwest Germany (Sauter, 1992) is shown in Fig. 2. The large peaks after each rain event are attributed to the fast flow through the enlarged fractures of the karst aquifer, which have a low storage capacity. The recession limbs are controlled by slow flow through the finer fissures of the rock matrix, which has a high storage capacity. Analysis of karst spring hydrographs is a common tool to study the response of a karst aguifer to groundwater flow (Atkinson et al., 1973; Sauter, 1992; Grasso and Jeannin, 1998; Baedke and Krothe, 2001; Jeannin, 2001). However, the hydrograph analyses are often limited by a number of factors, e.g. the large catchment of karst aquifers, the strong heterogeneities in conductivity, and the scarcity of data (see Jeannin and Sauter, 1998, for a review).

Besides analysis of a measured spring discharge hydrograph, hydrograph time-series can be generated by numerical flow models, which describe a karst aquifer geometry in a simplified fashion. This numerical approach excludes per definition uncertainties in the hydraulic properties, and thus can be used to study the response of a karst aquifer to recharge events. For example, Eisenlohr et al. (1997a,b) have used the numerical model of transient groundwater flow described in Király (1998), with flow driven by the rainfall time-series from the Areuse and Serrière catchments in the Swiss Jura. The finite-element model includes both low-flow, high-storage porous matrix, and high-flow, low-storage karst conduits into the approach. The resulting spring discharge was then analysed with an auto-correlation method, and it was shown that the recharge input (frequency and intensity of recharge events, infiltration,...) strongly controls the correlation functions.

The numerical prediction of karst spring hydrographs also showed that an important input parameter for a quantitative hydrograph analysis is the karst aquifer geometry. Here, assumptions need to be made concerning the location and distribution of enlarged fractures, as well as hydraulic properties for both the highly permeable fractures and the low-permeability porous matrix. Often, these data are not available from field observations, and simplified models have to be used instead. While Eisenlohr et al. (1997a,b) have assigned a constant conductivity to karst conduits, which where placed in the numerical model domain in an 'ad-hoc' fashion, we discuss another possibility to access the karst aquifer properties: we make use of numerically generated long-term karst aquifer models and simulate short-term transient flow behaviour driven by a realistic recharge times series. Our aim is to test synthetic karst aquifer models, which are calculated as evolution models under the assumption of steady-state recharge, under transient event-based recharge conditions. We predict spring discharge time-series and show that a long-term numerical karst evolution model is capable of describing the flashy response typical to mature karst aquifers.

The outline of the following study is as follows: in Section 2 we introduce the basic theory of calcite dissolution chemistry, and the

## Download English Version:

# https://daneshyari.com/en/article/4686543

Download Persian Version:

https://daneshyari.com/article/4686543

<u>Daneshyari.com</u>